RESEARCH

Testing the Amati and Yonetoku correlations for short gamma-ray bursts

Hannachi Zitouni[1] · Nidhal Guessoum[2] · Walid Azzam[3]

Abstract

We use a sample of *Swift* and *Fermi* short gamma-ray bursts (SGRBs) to test the validity of the Amati and Yonetoku correlations, which were originally found for long bursts. The first relation is between $E_{p,i}$, the intrinsic peak energy of the GRB prompt emission, and E_{iso}, the equivalent isotropic energy. The second relationship is between $E_{p,i}$ and L_{iso}, the peak isotropic luminosity. The sample is composed of 36 *Swift* SGRBs and 15 *Fermi* SGRBs that have measured redshifts and whose spectral parameters, with their uncertainties, are available online. The uncertainties (error bars) on the values of the calculated energy flux P, of the energy E_{iso}, and of the peak isotropic luminosity peak L_{iso} are estimated using a Monte Carlo approach.

We find that SGRB energy and luminosity quantities ($E_{p,i}$, L_{iso}, and E_{iso}) can be correlated with Amati- and Yonetoku-like relations reasonably well (Pearson r-values of 0.5 and 0.6, respectively), although the data shows large scatter and hence large error bars on the slope and the intercept of the fitting line. Our results are consistent with other similar works, though we here use the largest sample of SGRBs with redshifts so far on this topic. We also find that E_{iso} and L_{iso} seem to evolve with redshift as $(1+z)^{4.9\pm0.3}$ and $(1+z)^{5.5\pm0.9}$, respectively, with a moderate goodness of fit. However, we caution that this is probably due to selection effects rather than being a genuine redshift evolution of E_{iso} and L_{iso}.

1 Introduction

Gamma-ray bursts (GRBs), in addition to being remarkable phenomena (the most powerful explosions in the universe), inviting researchers to combine various physical aspects into potent models, provide astrophysicists and cosmologists with new tools to explore the universe. Indeed, while the precise mechanism behind these explosions has proven at least partially elusive, new opportunities, both observational (e.g. gravitational waves) and theoretical (e.g. correlation functions) have provided hopes for new breakthroughs. Moreover, GRBs give cosmologists great promise as potential probes of the early epochs of the universe, first because they have been observed up to very high redshift ($z > 9$, with upcoming satellites, particularly SVOM, promising data from even deeper regions/times), and their gamma-ray emission crosses billions of light-years without being affected.

The main problem with the cosmographic utility of GRBs, however, has been that they are not standard candles and thus cannot readily be used as cosmological tools (as Supernovae Ia are, for instance). For this reason, the discovery of correlations between physical parameters of GRBs (at least long ones) has been a boon. Two such correlations have been found: the Amati (2006) relation, between $E_{p,i}$, the intrinsic peak energy of a burst's prompt emission, and E_{iso}, the equivalent isotropic energy of the burst; the Yone-

All authors contributed equally to this work.

✉ H. Zitouni
zitouni.hannachi@univ-medea.dz

N. Guessoum
nguessoum@aus.edu

W. Azzam
wjazzam@uob.edu.bh

[1] Laboratoire PTEA, Faculté des sciences, Université Dr Yahia Fares, Pôle urbain, 26000, Médéa, Algeria

[2] Department of Physics, College of Arts & Sciences, American University of Sharjah, Sharjah, UAE

[3] Department of Physics, College of Science, University of Bahrain, Sakheer, Bahrain

toku et al. (2004) relation, between $E_{p,i}$ (as just defined) and L_{iso}, the isotropic peak luminosity. These correlations, and a few other similar ones, have been established (to some extent) for long bursts (those of duration longer than 2.0 seconds). Our work consists in investigating the (statistical) extent to which these relations also hold for short GRBs.

There are important implications to these investigations. First, as mentioned above, if established, such relations would be very valuable for cosmological studies, as they would provide constraints on, if not direct access to, physical characteristics of extremely distant cosmic objects. They would also help constrain the physical mechanisms and models for those powerful explosions: the hypernova collapses of the biggest stars in the universe, and the merger between compact objects (a neutron star with another one or with a black hole). And in the latter case, which then gives a short gamma-ray burst, this would tie in with gravitational waves (GW), such as the historic GW170817, with its GRB and kilonova counterparts, GRB170817A and AT2017gfo, respectively (Abbott et al. 2017a,b).

Studies of the Amati and Yonetoku relations focusing on short GRBs have been few and with small samples: Zhang and Mészàros (2004), Tsutsui et al. (2013b), Shahmoradi and Nemiroff (2015), Azzam et al. (2020). The reason for this limited amount of work is that energy and luminosity quantities, to be inferred from fluxes, require knowledge of distances, which means measurements of redshifts. Short GRBs only account for 9% to 25% of all bursts (9% of the *Swift* bursts, 16% of *Fermi*'s, and 25% of *BATSE*'s, as per the data available on these satellites' official websites), and of those an even smaller fraction gets a reliable redshift measurement. This situation has started to improve, and we now have a few dozen such cases, thus allowing for an improved statistical investigation, which is what we are undertaking in this work, especially with the multiple avenues that such knowledge promises to open for astrophysicists.

Following this introduction, Sect. 2 provides a full presentation of our sample selection; Sect. 3 then lays out our spectral analysis; Sect. 4 presents our results and findings; Sect. 5 provides a discussion and a comparison with previous works; and Sect. 6 gives our conclusions.

2 Sample selection

Our sample consists of 51 short gamma ray bursts (SGRBs) with measured redshifts, as shown in Table 1: 36 of those were detected by the *Swift* satellite and 15 by the *Fermi* satellite. The *Swift* website[1] gives 52 SGRBs with redshifts; however, we eliminated one of them (100628A) because of

the lack of spectral parameters for it. The spectral parameters of the 36 *Swift* SGRBs were obtained from the official *Swift* website,[2] while those of the 15 *Fermi* SGRBs were collected from the official *Fermi* data website.[3] Some data entries were checked against those of Minaev and Pozanenko (2019) and Iyyani and Sharma (2021).

Swift burst spectra are represented by a broken power law characterized by a single index, denoted here by α, and the peak energy denoted by E_p. The spectra of the *Fermi* bursts are represented by a Band function characterized by two indices, denoted here by α and β, and the energy at the peak, E_p.

For each burst we considered two types of spectra: the spectrum observed at the peak of the flux for a duration of one second (called resolved spectrum) and the spectrum averaged over the entire duration of the burst (called integrated spectrum). The difference between the two is due, on the one hand, to the calculation of the total isotropic energy, denoted E_{iso}, from the fluence and the average spectrum, and on the other hand, to the calculation of the isotropic luminosity relative to the peak of the flux for a duration of one second.

All the data used here are provided with their average values and their errors, with the exception of a few bursts that we mention below. The missing values concern the errors ΔE_p on the peak energy for the given type of spectrum. There are bursts which have $\Delta E_p = 0$, e.g. 051221A, 070809, 080905A, 090515, 140622A, 150120A, 161104A, and 170428A. In this case we assumed that the error is one tenth the average value instead of being set to zero. Other bursts have infinitely large ΔE_p, e.g. 050509B, 060801, 070729B, 090426, 120804A and 150120A. In this case we have assumed that the error is equal to the given mean value.

Figure 1(a) shows the distribution of the 51 SGRBs as a function of the redshift z. This distribution shows that the bursts that are most frequently observed are those that are closest to us. This may be due to the lack of sensitivity of the detectors to very low fluxes and to the very short durations of the bursts. We note that the *Swift* and *Fermi* bursts are similarly distributed in redshifts as well as in intrinsic duration, although the limited number of *Fermi* bursts produce some slight incongruities.

In Fig. 1(b), we show the distribution of the bursts in our sample according to the intrinsic duration $T_{90}^{obs}/(1+z)$. This distribution strongly resembles that of the first population of short bursts found by Zitouni et al. (2015) on *CGRO/BATSE* and *Swift*/BAT samples, thus giving credence to the sample used here.

Fig. 1 (**a**): Distribution of 51 SGRBs with redshift z, with a bin of 0.5, (**b**): Distribution of 51 SGRBs versus intrinsic duration $T_{90}^{obs}/(1+z)$, with a bin of 0.2
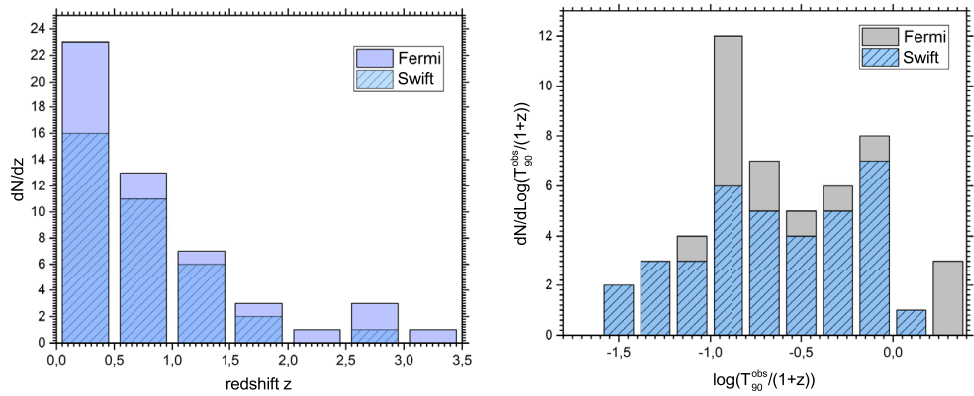
3 Spectral analysis

For the *Swift* bursts, the peak 1-sec photon flux, fluence, and spectral parameters are given for the energy band between $E_{min} = 15$ keV and $E_{max} = 350$ keV. As we previously mentioned, the spectral function is widely modeled as a broken power law, with a single index, noted α, and a parameter E_0:

$$N(E) = N_0 \left[\frac{E}{100 \text{ keV}} \right]^\alpha e^{-E/E_0}; \tag{1}$$

the spectral parameters E_0 ($E_0 = \frac{E_p^{obs}}{2+\alpha}$), α, and E_p^{obs} are given by the *Swift* data website.

GRB data from the *Fermi* telescope is given in the energy band from $E_{min} = 10$ keV to $E_{max} = 1000$ keV. The spectrum is often modeled by the Band function, which is characterized by a low energy index, noted α, and a high energy index, noted β:

$$\frac{N(E)}{N_0} = \begin{cases} \left[\frac{E}{100 \text{ keV}} \right]^\alpha e^{\frac{E}{E_0}}, & \frac{E}{E_0} \le (\alpha - \beta), \\ A \left[\frac{E}{100 \text{ keV}} \right]^\beta, & \frac{E}{E_0} \ge (\alpha - \beta), \end{cases} \tag{2}$$

with $A = \left[\frac{(\alpha-\beta)E_0}{100 \text{ keV}} \right]^{\alpha-\beta} e^{\beta-\alpha}$ and $E_0 = \frac{E_p^{obs}}{2+\alpha}$. The spectral parameters α, β and E_p^{obs} are given by the *Fermi* data website.

The peak energy flux, denoted by F_γ and calculated in erg cm^{-2} s^{-1}, is determined numerically using the following equation (Zitouni et al. (2014)):

$$F_\gamma = R \, P_{ph} \frac{\int_{E_{min}}^{E_{max}} E N(E) dE}{\int_{E_{min}}^{E_{max}} N(E) dE}. \tag{3}$$

A factor $R = 1.6 \times 10^{-9}$ is introduced to make the keV-erg conversion. P_{ph} is the flux (in photons cm^{-2} s^{-1}) tabulated in Table 1, column 7.

The maximum energy emitted per unit time over all space is the peak isotropic bolometric luminosity (over 1 second), designated as L_{iso}. The E.N(E) function is integrated in the energy band corresponding to the measured gamma radiation band in the source's frame, i.e. $E_1 = 1$ keV to $E_2 = 10^4$ keV. The equivalent measured energy band is $E_1/(1+z)$ to $E_2/(1+z)$, considering the cosmological relativistic effect.

Thus the k-corrected L_{iso} is calculated via:

$$L_{iso} = 4\pi d_L^2 \int_{E_1/(1+z)}^{E_2/(1+z)} E N(E) dE, \tag{4}$$

$$= 4\pi d_L^2 F_\gamma k_c. \tag{5}$$

Here L_{iso} is k-corrected with the method developed by Bloom et al. (2001) and given by:

$$k_c = \frac{\int_{E_1/(1+z)}^{E_2/(1+z)} E N(E) dE}{\int_{E_{min}}^{E_{max}} E N(E) dE}, \tag{6}$$

where k_c is the proper k-correction factor [Yonetoku et al. (2004), Rossi et al. (2008), Elliott et al. (2012b)].

These integrals are performed numerically using the time-resolved spectral parameters given by the *Swift* and *Fermi* data websites. The cosmological distance d_L is given by the following equation:

$$d_L = \frac{(1+z)c}{H_0} \int_0^z \frac{dz'}{\sqrt{\Omega_M(1+z')^3 + \Omega_L}}. \tag{7}$$

We adopt the following cosmological parameters: $\Omega_M = 0.27$, $\Omega_L = 0.73$, and $H_0 = 70$ km/s/Mpc (e.g. Komatsu et al. (2009)).

The total isotropic energy, denoted as E_{iso}, which is emitted by a gamma-ray burst over all space, is calculated using the fluences (erg/cm^2) given by the detectors in the energy band [15–350] keV for *Swift* and [10–1000] keV for *Fermi*. To calculate this, we use time-averaged spectral parameters (α_m, E_{pm}) obtained for the CPL spectrum from the *Swift*

Table 1 Data of 51 Short gamma ray bursts

Name	z	T_{90} (s)	Fluence (erg cm^{-2}) ($\times 10^{-7}$)	Flux (pho cm^{-2} s^{-1})	E_{pk}^{Obs} (keV)	E_{pm}^{Obs} (keV)	Exp	$\log(E_{iso})$ (erg)	$\log(L_{iso})$ (erg s^{-1})
211023B	0.862	1.3	1.9 ±0.731	2.24± 0.373	52.3 ± 1.3	47.0 ±1.3	Swift	50.66 ± 0.25	50.82 ± 0.11
201221D	1.046	0.16	4.7 ±1.17	5.89± 0.769	95.9 ± 33.1	87.6 ±79.1	Swift	53.32 ± 0.15	51.57 ± 0.09
200522A	0.4	0.62	1.2 ±0.379	1.52± 0.227	84.1 ± 113.7	77.8 ±52.6	Swift	49.83 ± 0.15	50.00 ± 0.16
190627A	1.942	1.6	0.914 ±0.39	1.08± 0.262	25.8 ± 17.9	24 ±17.9	Swift	50.96 ± 0.20	50.39 ± 0.15
160624A	0.483	0.2	1.54 ±1.72	0.933± 0.52	9999.4 ± 999.9	10000 ±1000	Swift	52.38 ± 0.58	51.98 ± 0.58
150424A	1.00	0.273	31.7 ±5.37	18.0± 1.30	9998.7 ± 999.8	9999.4 ±999.9	Swift	52.08 ± 0.51	52.43 ± 0.001
150423A	1.394	0.22	0.866 ±0.594	0.935± 0.324	125.8 ± 39.7	123.5 ±39.7	Swift	50.96 ± 0.23	51.23 ± 0.18
150120A	0.46	1.2	2.13 ±0.536	1.93± 0.168	357.3 ± 35.73	311.3 ±31.13	Swift	50.495 ± 0.14	50.50 ± 0.08
141212A	0.596	0.3	0.923 ±0.325	1.24± 0.265	74.7 ± 27.2	94.3 ±28.3	Swift	50.08 ± 0.16	50.22 ± 0.13
140903A	0.351	0.3	1.39 ±0.248	2.5 ± 0.228	40.4 ± 13.9	44.3 ±13.9	Swift	49.70 ± 0.11	49.98 ± 0.10
140622A	0.959	0.132	0.27 ±0.04	0.65± 0.255	46.4 ± 4.64	44.2 ±7.4	Swift	49.81 ± 0.12	50.38 ± 0.15
131004A	0.717	1.54	2.99 ±0.623	3.35± 0.246	63.4 ± 15.3	60.6 ±38.1	Swift	50.73 ± 0.13	50.86 ± 0.06
130603B	0.356	0.18	16.5 ±2.96	9.27± 0.736	9998.1 ± 999.8	999.8 ±99.98	Swift	51.68 ± 0.11	52.25 ± 0.19
120804A	1.30	0.808	17.2 ±1.49	13.1± 0.64	156.0 ± 156.0	156.1 ±156.1	Swift	52.31 ± 0.20	52.47 ± 0.20
101219A	0.718	0.6	14.2 ±1.65	6.43± 0.454	9999.4 ± 999.9	9999.4 ±999.9	Swift	53.23 ± 0.13	53.05 ± 0.13
100724A	1.288	1.4	1.43 ±0.341	1.81± 0.259	45.1 ± 9.4	42.4 ±11.7	Swift	50.77 ± 0.12	51.13 ± 0.09
090426	2.609	1.2	1.85 ±0.724	2.43± 0.389	60.8 ± 60.8	49.3 ±49.3	Swift	52.12 ± 0.35	52.54 ± 0.19
080905A	0.1218	1.0	3.46 ±1.69	1.83± 0.3	855.8 ± 85.5	499.3 ±49.9	Swift	49.72 ± 0.23	49.71 ± 0.25
071227	0.383	1.8	7.83 ±4.76	2.08± 0.301	9999.3 ± 5000	57.5 ±5.75	Swift	50.65 ± 0.21	52.32 ± 0.02
070809	0.2187	1.21	1.34 ±0.55	1.38± 0.221	279.0 ± 27.9	262.8 ±5000.0	Swift	51.80 ± 0.31	51.96 ± 0.11
070714A	0.90	2.00	10.6 ±6.08	3.93± 0.265	129.6 ± 12.96	9998.8 ±5000.0	Swift	52.50 ± 0.61	51.30 ± 0.04
070729	0.80	0.980	1.88 ±1.21	1.20± 0.38	248.1 ± 248.1	202.2 ±202.2	Swift	51.21 ± 0.55	51.15 ± 0.40
070724A	0.457	0.4	0.471 ±0.165	0.792± 0.152	41.2 ± 4.12	41.2 ±4.12	Swift	49.50 ± 0.13	49.78 ± 0.08
070429B	0.904	0.47	0.665 ±0.338	1.78± 0.303	65.1 ± 65.1	66.7 ±65.1	Swift	50.38 ± 0.19	50.90 ± 0.14
061217	0.827	0.21	0.792 ±0.424	2.42± 0.458	9997.2 ± 5000	9997.2 ±5000	Swift	51.82 ± 0.37	52.48 ± 0.42
061201	0.111	0.76	4.29 ±1.49	5.76± 0.508	873.0 ± 458	873 ±458	Swift	49.94 ± 0.25	50.06 ± 0.20
060801	1.130	0.504	1.38 ±0.138	2.27± 0.364	210.4 ± 210.4	196.3 ±196.3	Swift	52.24 ± 0.80	52.69 ± 0.52
060502B	0.287	0.131	0.458 ±0.287	3.09± 0.596	102 ± 101.8	97.5 ±77.3	Swift	49.18 ± 0.26	50.07 ± 0.22
051221A	0.547	1.4	13.6 ±0.349	14.5± 0.831	524.9 ± 52.49	840.9 ±84.0	Swift	51.66 ± 0.06	51.70 ± 0.06
050813	1.8	0.45	0.404 ±0.212	0.874± 0.236	60.4 ± 32.4	65.9 ±48.8	Swift	50.65 ± 0.24	51.26 ± 0.20
050509B	0.225	0.073	0.0891 ±0.0404	1.88± 0.478	69.4 ± 69.4	69.7 ±69.7	Swift	48.28 ± 0.31	49.66 ± 0.23
170428A	0.454	0.200	6.14 ±2.34	3.83 ±0.577	409.7 ±40.97	298.5 ±29.85	Swift	50.98±0.15	50.98± 0.124
161104A	0.788	0.100	0.328 ±0.0733	0.704 ±0.188	9999.0 ±999.9	65.7 ±21.1	Swift	49.79±0.15	51.25±0.42
090417A	0.088	0.068	0.189 ±0.0502	4.28 ±1.14	41.0 ±12.4	40.3 ±12.8	Swift	47.47±0.18	48.75±0.15
070923	0.076	0.040	1.1 ±0.0862	3.31 ±0.58	9991.8 ±5000.0	9999.0 ±5000.0	Swift	49.72±0.02	50.15±0.41
090515	0.403	0.036	0.253 ±0.0889	0.329 ±0.193	138.8 ±13.88	79.8 ±56.6	Swift	49.13±0.26	49.48±0.21
160821B	0.16	1.088	1.95 ±0.202	8.554± 1.17	125.19 ± 75.88	38.17 ±27.48	Fermi	49.06 ± 0.0012	50.13 ± 0.08
160624A	0.483	0.384	3.92 ±0.085	6.004± 0.83	677.74 ± 257.	1168.4 ±546.	Fermi	51.47 ± 0.31	51.50 ± 0.08
150101A	0.093	0.080	2.38 ±0.151	9.82± 1.39	22.70 ± 3.73	28.67 ±6.74	Fermi	48.72 ± 0.05	50.46 ± 0.34
150120A	0.460	3.328	3.35 ±0.217	4.664± 4.664	10.43 ± 10.43	15.56 ±15.56	Fermi	51.59 ± 0.04	53.24 ± 0.05
140619B	2.67	0.448	2.10 ±0.438	11.77± 2.09	307.90 ± 77.4	243.93 ±52.11	Fermi	51.59 ± 0.04	53.24 ± 0.05
111117	2.21	0.432	5.64 ±0.128	9.774± 9.68	287.51 ± 49.88	502.85 ±111.18	Fermi	52.17 ± 0.04	53.06 ± 0.19
100625	0.452	0.240	5.63 ±0.245	17.04± 2.26	364.84 ± 214.01	482.13 ±61.94	Fermi	50.75 ± 0.02	51.64 ± 0.09
100206	0.408	0.176	7.57 ±0.105	24.73± 1.35	566.48 ± 115.56	454.0 ±63.63	Fermi	50.44 ± 0.02	50.41 ± 0.04
100117A	0.915	0.256	4.23 ±0.693	8.125± 1.22	253.03 ± 71.0	327.22 ±52.92	Fermi	51.20 ± 0.04	51.90 ± 0.05

Table 1   (*Continued*)

Name	z	T_{90} (s)	Fluence (erg cm^{-2}) ($\times 10^{-7}$)	Flux (pho cm^{-2} s^{-1})	E_{pk}^{Obs} (keV)	E_{pm}^{Obs} (keV)	Exp	log(E_{iso}) (erg)	log(L_{iso}) (erg s^{-1})
090510	0.903	0.960	33.73 ±0.406	42.4± 1.764	2632.9 ± 306.	4248.1 ±440.	*Fermi*	52.86 ± 0.01	53.42 ± 0.02
090227	1.61	0.304	1.11 ±0.119	126.8± 2.75	2021.9 ± 90.75	2095.2 ±99.82	*Fermi*	52.86 ± 0.01	53.42 ± 0.02
090426	2.609	7.488	35.38 ±0.882	6.124± 0.28	295.1 ± 87.5	292.2 ±71.	*Fermi*	52.73 ± 0.02	52.73 ± 0.02
081024	3.05	0.640	3.55 ±0.286	5.714± 0.87	1446.4 ± 661.44	1757.4 ±1011.5	*Fermi*	52.40 ± 0.06	53.59 ± 0.07
170817A	0.009	2.048	2.79 ±0.174	2.94 ±0.76	176.96 ±98.8	214.7 ±56.60	*Fermi*	50.64±1.33	47±0.13
090927	1.37	0.512	3.026 ±0.183	5.06 ±1.017	97.37 ±15.14	195.22 ±69.05	*Fermi*	51.85±0.39	52.65±0.39

data and (α_m, β_m, E_{pm}) obtained for the Band spectrum from the *Fermi* data. The fluence S_{obs} is given in Table 1, column 4. Thus,

$$E_{iso} = \frac{4\pi d_L^2}{1+z} \int_{E_1/(1+z)}^{E_2/(1+z)} E\, N(E) dE,$$

$$= \frac{4\pi d_L^2}{1+z} S_{obs} k_c'. \tag{8}$$

k_c' is the cosmological k-correction as defined in Bloom et al. (2001) and $(1+z)$ is introduced to account for cosmological time dilation: $T_{90}^s = T_{90}^{obs}/(1+z)$ as defined in (Amati et al. (2002a), Hakkila et al. (2003), Gehrels et al. (2006), Elliott et al. (2012a), Atteia et al. (2018), Tu (2018), Dainotti and Amati (2018)). Similarly, $E_1/(1+z)$ to $E_2/(1+z)$ is the energy band in the source frame, with $E_1 = 1$ keV and $E_2 = 10^4$ keV.

It is important to note that we have accounted for all the uncertainties of the data as given in the *Swift* and *Fermi* databases. To evaluate the errors on the calculated quantities (L_{iso} and E_{iso}), we have used the Monte Carlo method assuming that each data value obeys the normal distribution, $\mathcal{N}(\mu, \sigma^2)$, with μ and σ are, respectively, the mean value and its uncertainty, both given in the data Table 2. For the fitting of the data and determination of the slopes and the intercepts in the relations between E_p and E_{iso} or L_{iso}, we used York's method (York 1966, 1968; York et al. 2004), which takes into account the errors (X-error and Y-error).

4 Results

4.1 The Amati $E_{iso} - E_{p,i}$ relation

The relation between the energies $E_{p,i}$ and E_{iso}, discovered by Amati et al. (2002b) has been the subject of numerous publications. This relation requires redshift measurements in order to determine the intrinsic properties of the source, as the intrinsic peak energy is given by the relation:

$$E_{p,i} = E_p^{obs} \times (1+z), \tag{9}$$

Table 2 $E_{iso} - E_{p,i}$ correlation. Ref1: Amati et al. (2002b), Ref2: Zitouni et al. (2014), Ref3: Shahmoradi (2013a,b), Ref4: Minaev and Pozanenko (2019)

	LGRBs			SGRBs	
	Ref1	Ref2	Ref3	Ref4	This work
K	95	141^{+18}_{-15}	–	2042 ± 47	1380^{+134}_{-121}
m	0.5	0.45 ± 0.10	0.25 ± 0.05	0.45 ± 0.03	0.47 ± 0.12

	36 *Swift* SGRBs	15 *Fermi* SGRBs
K	1325^{+611}_{-418}	1413^{+609}_{-426}
m	0.35 ± 0.13	0.56 ± 0.24

where E_p^{obs} is the peak energy measured by a given detector. The (fitting) Amati relation is then found to be of the form:

$$\frac{E_{p,i}}{\text{keV}} = K \times \left(\frac{E_{iso}}{10^{52}\,\text{erg}} \right)^m \tag{10}$$

where K and m are fitting constants.

For the original Amati relation (Amati et al. (2002b)), which was for long GRBs, $K \approx 95$ and $m \approx 0.5$. The most important parameter in this correlation function is the slope m. We are here mainly interested in this parameter. In Table 2, a comparison is made between the Amati parameters obtained for long and short bursts with those from this work, that is for short bursts. We show the values we obtain for our *Swift* and *Fermi* bursts separately and combined, as indeed we find no difference between the two sub-samples in either K or m to within 1σ. We also graphically represent, in Fig. 2, the variation of the intrinsic peak energy E_p as a function of E_{iso} for the 51 short bursts studied here.
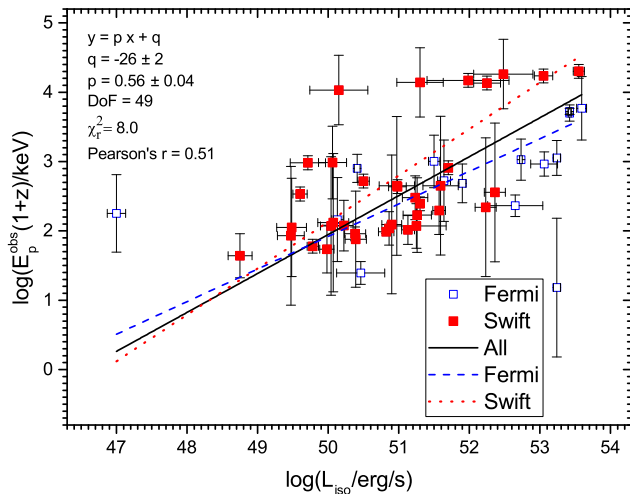
4.2 The Yonetoku $E_{p,i} - L_{iso}$ relation

The relation between the intrinsic peak energy $E_{p,i}$ and the isotropic luminosity at peak time, for bursts with well-determined redshifts, was found by Yonetoku et al. (2004).
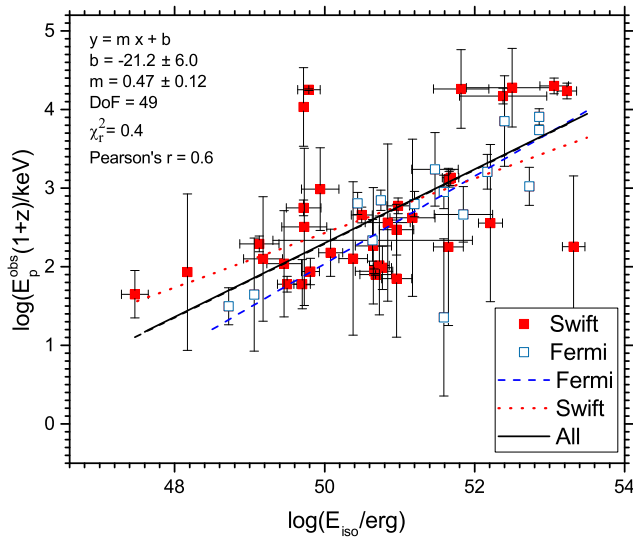
Fig. 2 The $E_{iso} - E_{p,i}$ correlation using 36 *Swift* + 15 *Fermi* SGRBs with well-determined redshifts and sufficient spectral data

Fig. 3 The $E_{p,i} - L_{iso}$ correlation using 36 *Swift* + 15 *Fermi* SGRBs with well-determined redshifts and sufficient spectral data

It was expressed as:

$$\frac{E_{p,i}}{1 \text{ keV}} = A \left(\frac{L_{iso}}{10^{52} \text{ ergs}} \right)^p \tag{11}$$

In Fig. 3 we plot $E_{p,i}$ vs. L_{iso} in log-log scale for 36 *Swift* bursts and 15 *Fermi* bursts with well determined redshifts and sufficient spectral data. In Table 3 we give the slope or power p in the Yonetoku relation (Eq. (11)) that we have obtained and compare it to both the results of Tsutsui et al. (2013a) for SGRBs and those of Yonetoku et al. (2004) and Zitouni et al. (2014) for LGRBs. Here again our combined-sample results are consistent with the previous works to within 1σ, and the two sub-samples are consistent with each other to within 1.5σ.

Table 3 $E_{p,i} - L_{iso}$ correlation. Ref1: Yonetoku et al. (2004), Ref2: Zitouni et al. (2014), Ref3: Shahmoradi (2013a), Osborne et al. (2020), Ref4: Tsutsui et al. (2013a), Ref5: Shahmoradi and Nemiroff (2015)

	LGRBs		
	Ref1	Ref2	Ref3,5
$\log A$	$-3.30^{+0.34}_{-0.36}$	$-3.08^{+1.22}_{-1.73}$	–
p	0.51 ± 0.05	$0.49^{+0.10}_{-0.07}$	0.27

	SGRBs				
	Ref4	Ref5	Our full sample	36 *Swift* bursts	15 *Fermi* bursts
$\log A$	8.2 ± 1.2	–	$3.00^{+0.46}_{-0.22}$	3.47 ± 0.40	2.58 ± 0.01
p	0.63 ± 0.04	0.8	0.56 ± 0.04	0.67 ± 0.20	0.47 ± 0.12

4.3 Selection effect on E_{iso} and L_{iso} at high z

Gamma-ray bursts are not immune to selection effects since the observational sample may not reflect the underlying "true" population correctly enough. As detailed in Dainotti and Amati (2018), these selection effects may involve the peak energy, the isotropic energy, the peak luminosity, or the isotropic luminosity. This is one of the main reasons that these (and other) correlation relations are controversial; indeed, their validity is questioned, due to the influence of several types of selection effects introduced by detector characteristics, sample incompleteness, and other such effects. Another selection effect, called "redshift desert" and introduced by Palmerio and Daigne (2021), is due to the fact that the most common emission and absorption lines are shifted out of the window of optical spectrographs at around $z \sim 2$. These selection effects have been extensively discussed: Band and Preece (2005), Ghirlanda et al. (2005), Nakar and Piran (2005), Butler et al. (2007), Bosnjak et al. (2008), Ghirlanda et al. (2008, 2012), Nava et al. (2008), Amati et al. (2009), Kocevski (2012), Butler et al. (2009), Krimm et al. (2009), Shahmoradi and Nemiroff (2009, 2010, 2011a,b), Shahmoradi (2013a), Shahmoradi and Nemiroff (2015), Heussaff et al. (2013), Mochkovitch and Nava (2015), Dainotti et al. (2016), Dainotti and Amati (2018), Osborne et al. (2020), Palmerio and Daigne (2021).

Some researchers argue that the Amati, Yonetoku, and other such correlations are caused by selection effects (Band and Preece (2005), Nakar and Piran (2005), Butler et al. (2007), Shahmoradi and Nemiroff (2010, 2011b), Heussaff et al. (2013)), while others argue that selection effects are insufficient to explain the observed correlation (Nava et al. (2008), Ghirlanda et al. (2008, 2012)).

A non-parametric statistical technique was developed early on by Efron and Petrosian (1992) to account for selection biases caused by GRB data truncation due to the detection threshold limit, which may affect the flux, the fluence, or the peak energy. This technique was further developed by
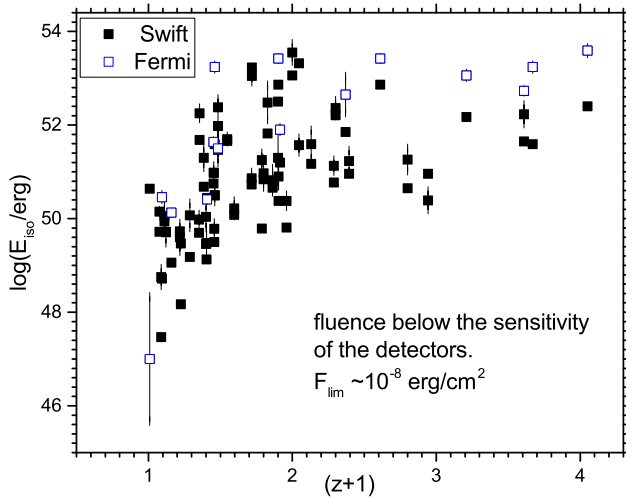
Fig. 4 Apparent redshift evolution of E_{iso} for the 51 SGRBs in our sample

Fig. 5 Apparent redshift evolution of L_{iso} for the 51 SGRBs in our sample

Lloyd and Petrosian (1999) and then utilized by Lloyd et al. (2000) to provide convincing evidence that there is an intrinsic correlation between the peak energy and the isotropic energy. It is worth noting that these studies preceded the official "discovery" of the Amati relation in 2002. Moreover, the fact that various instruments with different detection sensitivities and limits show a similar correlation is, to first order, a reassuring indicator that instrumental selection effects are not dominant. A similar argument can be made for the Yonetoku correlation.

We believe that this debate can only be resolved by the development of very sensitive detectors capable of covering a wide band of photon energies, as well as extensive observations that will produce a large sample of bursts with well determined redshifts.

In the sample of 51 SGRBs, we find an interesting selection effect of the isotropic energy E_{iso} in terms of the redshift z. We plot the data in Fig. 4, showing a trend between E_{iso} and $1 + z$. This can be explained by considering the selection effect of the GRBs found at high z and low luminosity, because the threshold of the fluence of the *Swift* and *Fermi* detectors is of the order of 10^{-8} erg cm^{-2}.

We also find a similar trend between L_{iso} and z (Fig. 5), a trend that may be due to the selection effect because the flux threshold of the *Swift* and *Fermi* detectors is of the order of 0.5 photons cm^{-2} s^{-1}.

For the sample of SGRBs considered in this study, our results can be summed up in the following points:

1. We obtain a good best-fit for the $E_{iso}-E_{p,i}$ correlation with a Pearson r-value of 0.58 and a reduced chi-square of 0.40. We obtain (Table 2) a best-fit slope $m = 0.47 \pm 0.12$, which is very close to and consistent (at the 1σ level) with the slope obtained by Minaev and Pozanenko (2019) for SGRBs, as well as with the slope for
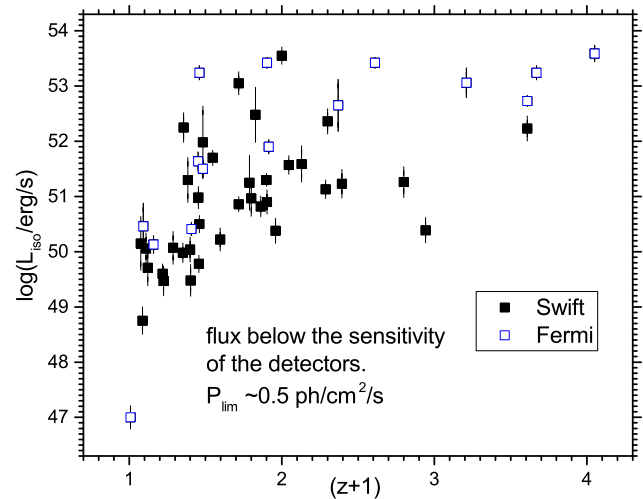
LGRBs obtained in both Amati's original study (Amati et al. (2002b)) and in our earlier study (Zitouni et al. (2014)). We also find no difference between *Swift* and *Fermi* bursts fitting parameters within 1σ.

2. We obtain a moderate best-fit for the $E_{p,i}$- L_{iso} correlation with a Pearson r-value of 0.51 and a reduced chi-square of 8.0. We obtain (Table 3) a best-fit slope $p = 0.56 \pm 0.04$, which is very close to and consistent (at the 1σ level) with the slope obtained by Tsutsui et al. (2013a) for SGRBs, and also with the slope for LGRBs obtained both in Yonetoku's original study (Yonetoku et al. (2004)) and in our earlier study (Zitouni et al. (2014)). Again we find the fitting values obtained with *Swift* and *Fermi* bursts to be consistent with one another within 1.5σ.

3. We find that E_{iso} evolves with the redshift, but this must be a selection effect due to the reduced detection of bursts at high redshift. Indeed, the low E_{iso} of GRBs coming from a source located at high redshift have a fluence below the detection limit of the detectors ($F_{limit} \sim 10^{-8}$ erg cm^{-2} for *Swift*/BAT and $\sim 2.5 \times 10^{-8}$ erg cm^{-2} for *Fermi*/GBM).

4. We also find that L_{iso} seems to evolve with the redshift. However, this is not for the same reason as E_{iso}. A selection effect due to detection limits filters out GRBs from places with high redshift, thus weak fluxes at the peak, making them undetectable (*Swift*: $P_{ph} < 0.6$ photons cm^{-2} s^{-1}; *Fermi*: < 0.5 photons cm^{-2} s^{-1}).

5 Discussion

Until recently, studies involving GRB energy and luminosity correlations have mostly been limited to LGRBs. This

is because these correlations require knowledge of the redshift, and the number of SGRBs with known redshift has been small. However, as more SGRBs with measured redshifts have become known in recent years, more attention has been given to the question of whether these correlations apply to SGRBs as well.

In this section, we provide a brief review of recent studies that have explored the degree to which the Amati and Yonetoku relations apply to SGRBs in order to put our study in proper context. One of the earliest studies to explore this issue is that by Zhang and Mészàros (2004). These authors used a sample of 17 SGRBs and 148 LGRBs to investigate the Yonetoku relation (only). They found that both SGRBs and LGRBs follow the Yonetoku relation with a best-fit given by: $E_{p,i} \propto L_{iso}^{0.59}$, which is consistent to within 1σ with what we find for the power index, $p = 0.56 \pm 0.04$.

The study by Tsutsui et al. (2013b) is especially relevant to our current paper because it explored both the Amati and Yonetoku correlations for SGRBs only. The study started by clarifying the occasionally ambiguous issue of when a GRB is to be considered short. The authors distinguished between what they called "secure" and "misguided" short bursts. (In two previous works we had explored the issue of GRB durations, observed and intrinsic, and the classification of bursts as 'short' or 'long', or possibly 'intermediate': Zitouni et al. (2015) and Zitouni et al. (2018).) Starting with a sample of 13 bursts, Tsutsui et al. (2013b) found that only 8 were "secure". They used these 8 bursts to obtain good fits for both the Amati and Yonetoku relations. However, they noted that for a given peak energy, L_{iso} is dimmer by a factor of about 5, and E_{iso} is dimmer by a factor of about 100, compared to the values of the same quantities for LGRBs.

A similar study, conducted by Shahmoradi and Nemiroff (2015), use the entire catalog of 600 CGRO/BATSE SGRBs to quantify the SGRB gamma-ray emission correlations, including the Amati and Yonetoku relations. Notably, they used Bayesian marginalization to circumvent the lack of knowledge of the redshifts of the entire BATSE catalog SGRBs and validated their results using a sample of 8 *Swift/Fermi* SGRBs. They obtained good fits for both correlations with a Peason correlation r-value of 0.60 ± 0.06 for the Amati relation and of 0.51 ± 0.10 for the Yonetoku relation (same as we obtained with our larger sample).

The recent study by Azzam et al. (2020) used a sample of 18 SGRBs and 49 LGRBs to explore the Amati correlation (only). These authors applied a log fit of the form: $\log(\frac{E_{iso}}{erg}) = A + B \times \log(\frac{E_{p,i}}{<E_{p,i}>})$ where $<E_{p,i}>$ is the mean intrinsic peak energy of the sample, and A (normalization) and B (slope) are fitting parameters. The authors obtained good fits for both samples of short and long bursts with a linear regression coefficient, r, of 0.86 and 0.67, for SGRBs and LGRBs, respectively. The authors also found that the slope B for the short and long bursts are consistent with one another to within 1σ, but that the normalization A for SGRBs is about two orders of magnitude lower than that of LGRBs, which is not surprising since the total energy of SGRBs is considerably less than that of LGRBs.

Our current investigation agrees with the above studies in that it confirms the conformity of the short bursts to both the Amati and Yonetoku correlations. Moreover, our study, as far as we are aware, uses the largest available (and relevant) sample of SGRBs to concurrently investigate the Amati and Yonetoku correlations while incorporating the observational uncertainties in the data, unlike the recent study by Azzam et al. (2020), which although it used a sample of 18 SGRBs (compared to 51 here), did not incorporate these observational uncertainties.

Our most interesting result is the fact that the slopes (or power indices) of both the Amati and the Yonetoku relations found in this work are not only very close and consistent with the works on short bursts that have preceded us, but furthermore to within 1-sigma are also consistent with the slopes obtained for long bursts (where the samples are much larger). However, our intercepts (or normalization factors) differ from others' by 4 or 5 sigmas, and this we believe is due to the large scatter in the data; hopefully, future measurements will have smaller uncertainties and more accurate values, and should bring all results within 1 or 2 sigma of each other.

6 Conclusion

The availability of more extensive data on short GRBs, particularly redshift measurements but also spectra parameters, is now allowing us to test relations such as Amati's and Yonetoku's, as well as dependence/evolution of physical parameters such as the isotropic energy and luminosity of a burst on/with redshift. This helps explore issues of detection limits and their impact on data and inferred parameters, as well as spectral and physical models of bursts. The data is still somewhat plagued by large uncertainties, which translates into high variation in some of the fitting parameters, particularly the intercepts.

With a sample of 51 bursts, we have not only confirmed others' results, which had been obtained with much smaller samples, but also found interesting similarity and consistency of the fitting parameters with those of long bursts.

Finally, we stress again the importance of focusing on short bursts, as they tie in with GW detections in the era of multi-messenger astronomy. Indeed, there has so far been only one case of a short burst associated with a GW detection (that of Aug. 17, 2017), where two neutron stars merged and produced signals across the entire electromagnetic spectrum (thus observable from the ground and from space) as well as gravitational waves. Many more are expected in the

next few years, as the GW facilities are being upgraded, thus multi-pronged analyses and characterizations of short bursts will be highly valuable. This work is a step in that direction.

Declarations

Conflict of interest The authors have no relevant financial or non-financial interests to disclose.

Competing interests The authors declare no competing interests.

References

Abbott, B.P., et al.: Phys. Rev. Lett. **119**(16), 161101 (2017a). https://doi.org/10.1103/PhysRevLett.119.161101.

Abbott, B.P., et al.: Astrophys. J. **848**(2), L13 (2017b). https://doi.org/10.3847/2041-8213/aa920c.

Amati, L.: Mon. Not. R. Astron. Soc. **372**, 233 (2006). https://doi.org/10.1111/j.1365-2966.2006.10840.x

Amati, L., Frontera, F., Tavani, M., in't Zand, J.J.M., Antonelli, A., Costa, E., Feroci, M., Guidorzi, C., Heise, J., Masetti, N., Montanari, E., Nicastro, L., Palazzi, E., Pian, E., Piro, L., Soffitta, P.: Astron. Astrophys. **390**, 81 (2002a). https://doi.org/10.1051/0004-6361:20020722. arXiv:astro-ph/0205230

Amati, L., Frontera, F., Tavani, M., in't Zand, J.J.M., Antonelli, A., Costa, E., Feroci, M., Guidorzi, C., Heise, J., Masetti, N., Montanari, E., Nicastro, L., Palazzi, E., Pian, E., Piro, L., Soffitta, P.: Astron. Astrophys. **390**, 81 (2002b). https://doi.org/10.1051/0004-6361:20020722

Amati, L., Frontera, F., Guidorzi, C.: Astron. Astrophys. **508**(1), 173 (2009). https://doi.org/10.1051/0004-6361/200912788. arXiv:0907.0384

Atteia, J.-L., Heussaff, V., Dezalay, J.-P., Klotz, A., Turpin, D., Tsvetkova, A.E., Frederiks, D.D., Zolnierowski, Y., Daigne, F., Mochkovitch, R.: Astrophys. J. **852**(2), 144 (2018). https://doi.org/10.3847/1538-4357/aaa414

Azzam, W.J., Jaber, F.S., Ambareena, N.: J. Appl. Math. Phys. **8**(11) (2020). https://doi.org/10.4236/jamp.2020.811175

Band, D.L., Preece, R.D.: Astrophys. J. **627**(1), 319 (2005). https://doi.org/10.1086/430402. arXiv:astro-ph/0501559

Bloom, J.S., Frail, D.A., Sari, R.: Astron. J. **121**, 2879 (2001). https://doi.org/10.1086/321093. arXiv:astro-ph/0102371

Bosnjak, Z., Celotti, A., Longo, F., Barbiellini, G.: Mon. Not. R. Astron. Soc. **384**(2), 599 (2008). https://doi.org/10.1111/j.1365-2966.2007.12672.x. https://academic.oup.com/mnras/article-pdf/384/2/599/3394281/mnras0384-0599.pdf

Butler, N.R., Kocevski, D., Bloom, J.S., Curtis, J.L.: Astrophys. J. **671**(1), 656 (2007). https://doi.org/10.1086/522492. arXiv:0706.1275

Butler, N.R., Kocevski, D., Bloom, J.S.: Astrophys. J. **694**(1), 76 (2009). https://doi.org/10.1088/0004-637x/694/1/76

Dainotti, M.G., Amati, L.: Publ. Astron. Soc. Pac. **130**(987), 051001 (2018). https://doi.org/10.1088/1538-3873/aaa8d7. arXiv:1704.00844

Dainotti, M., Del Vecchio, R., Tarnopolski, M.: arXiv e-prints, 1612 (2016). arXiv:1612.00618

Efron, B., Petrosian, V.: Astrophys. J. **399**, 345 (1992). https://doi.org/10.1086/171931

Elliott, J., Greiner, J., Khochfar, S., Schady, P., Johnson, J.L., Rau, A.: Astron. Astrophys. **539**, 113 (2012a). https://doi.org/10.1051/0004-6361/201118561. arXiv:1202.1225

Elliott, J., Greiner, J., Khochfar, S., Schady, P., Johnson, J.L., Rau, A.: Astron. Astrophys. **539**, 113 (2012b). https://doi.org/10.1051/0004-6361/201118561. arXiv:1202.1225

Gehrels, N., Norris, J.P., Barthelmy, S.D., Granot, J., Kaneko, Y., Kouveliotou, C., Markwardt, C.B., Mészáros, P., Nakar, E., Nousek, J.A., O'Brien, P.T., Page, M., Palmer, D.M., Parsons, A.M., Roming, P.W.A., Sakamoto, T., Sarazin, C.L., Schady, P., Stamatikos, M., Woosley, S.E.: Nature **444**(7122), 1044 (2006). https://doi.org/10.1038/nature05376. arXiv:astro-ph/0610635

Ghirlanda, G., Ghisellini, G., Firmani, C., Celotti, A., Bosnjak, Z.: Mon. Not. R. Astron. Soc. **360**, 45 (2005). https://doi.org/10.1111/j.1745-3933.2005.00043.x

Ghirlanda, G., Nava, L., Ghisellini, G., Firmani, C., Cabrera, J.I.: Mon. Not. R. Astron. Soc. **387**(1), 319 (2008). https://doi.org/10.1111/j.1365-2966.2008.13232.x. https://academic.oup.com/mnras/article-pdf/387/1/319/3206286/mnras0387-0319.pdf

Ghirlanda, G., Ghisellini, G., Nava, L., Salvaterra, R., Tagliaferri, G., Campana, S., Covino, S., D'Avanzo, P., Fugazza, D., Melandri, A., Vergani, S.D.: Mon. Not. R. Astron. Soc. **422**(3), 2553 (2012). https://doi.org/10.1111/j.1365-2966.2012.20815.x. arXiv:1203.0003

Hakkila, J., Giblin, T.W., Roiger, R.J., Haglin, D.J., Paciesas, W.S., Meegan, C.A.: Astrophys. J. **582**(1), 320 (2003). https://doi.org/10.1086/344568. arXiv:astro-ph/0209073

Heussaff, V., Atteia, J.-L., Zolnierowski, Y.: Astron. Astrophys. **557**, 100 (2013). https://doi.org/10.1051/0004-6361/201321528. 15 pages, 5 figures, same version as the paper published in Astron. Astrophys.

Iyyani, S., Sharma, V.: Astrophys. J. Suppl. Ser. **255**(2), 25 (2021). https://doi.org/10.3847/1538-4365/ac082f

Kocevski, D.: Astrophys. J. **747**(2), 146 (2012). https://doi.org/10.1088/0004-637x/747/2/146

Komatsu, E., Dunkley, J., Nolta, M.R., Bennett, C.L., Gold, B., Hinshaw, G., Jarosik, N., Larson, D., Limon, M., Page, L., Spergel, D.N., Halpern, M., Hill, R.S., Kogut, A., Meyer, S.S., Tucker, G.S., Weiland, J.L., Wollack, E., Wright, E.L.: Astrophys. J. Suppl. Ser. **180**, 330 (2009). https://doi.org/10.1088/0067-0049/180/2/330. arXiv:0803.0547

Krimm, H.A., Yamaoka, K., Sugita, S., Ohno, M., Sakamoto, T., Barthelmy, S.D., Gehrels, N., Hara, R., Norris, J.P., Ohmori, N., Onda, K., Sato, G., Tanaka, H., Tashiro, M., Yamauchi, M.: Astrophys. J. **704**(2), 1405 (2009). https://doi.org/10.1088/0004-637x/704/2/1405

Lloyd, N.M., Petrosian, V.: Astrophys. J. **511**(2), 550 (1999). https://doi.org/10.1086/306719

Lloyd, N.M., Petrosian, V., Mallozzi, R.S.: Astrophys. J. **534**(1), 227 (2000). https://doi.org/10.1086/308742

Minaev, P.Y., Pozanenko, A.S.: Mon. Not. R. Astron. Soc. **492**(2), 1919 (2019). https://doi.org/10.1093/mnras/stz3611. https://academic.oup.com/mnras/article-pdf/492/2/1919/31838467/stz3611.pdf

Mochkovitch, R., Nava, L.: Astron. Astrophys. **577**, 31 (2015). https://doi.org/10.1051/0004-6361/201424490. arXiv:1412.5807

Nakar, E., Piran, T.: Mon. Not. R. Astron. Soc. **360**(1), 73 (2005). https://doi.org/10.1111/j.1745-3933.2005.00049.x. arXiv:astro-ph/0412232

Nava, L., Ghirlanda, G., Ghisellini, G., Firmani, C.: Mon. Not. R. Astron. Soc. **391**(2), 639 (2008). https://doi.org/10.1111/j.1365-2966.2008.13758.x. arXiv:0807.4931

Osborne, J.A., Shahmoradi, A., Nemiroff, R.J.: Astrophys. J. **903**(1), 33 (2020). https://doi.org/10.3847/1538-4357/abb9b7

Palmerio, J.T., Daigne, F.: Astron. Astrophys. **649**, 166 (2021). https://doi.org/10.1051/0004-6361/202039929. arXiv:2011.14745

Rossi, F., Guidorzi, C., Amati, L., Frontera, F., Romano, P., Campana, S., Chincarini, G., Montanari, E., Moretti, A., Tagliaferri, G.: Mon. Not. R. Astron. Soc. **388**, 1284 (2008). https://doi.org/10.1111/j.1365-2966.2008.13476.x. arXiv:0802.0471

Shahmoradi, A.: Astrophys. J. **766**(2), 111 (2013a). https://doi.org/10.1088/0004-637X/766/2/111. arXiv:1209.4647

Shahmoradi, A.: arXiv e-prints, 1308 (2013b). arXiv:1308.1097

Shahmoradi, A., Nemiroff, R.: In: Meegan, C., Kouveliotou, C., Gehrels, N. (eds.) Gamma-Ray Burst: Sixth Huntsville Symposium. American Institute of Physics Conference Series, vol. 1133, p. 425 (2009). https://doi.org/10.1063/1.3155940

Shahmoradi, A., Nemiroff, R.J.: Mon. Not. R. Astron. Soc. **407**(4), 2075 (2010). https://doi.org/10.1111/j.1365-2966.2010.16793.x. https://academic.oup.com/mnras/article-pdf/407/4/2075/17324824/mnras0407-2075.pdf

Shahmoradi, A., Nemiroff, R.J.: In: American Astronomical Society Meeting Abstracts. American Astronomical Society Meeting Abstracts, vol. 217, p. 249 (2011a)

Shahmoradi, A., Nemiroff, R.: Mon. Not. R. Astron. Soc. **411**(3), 1843 (2011b)

Shahmoradi, A., Nemiroff, R.J.: Mon. Not. R. Astron. Soc. **451**(1), 126 (2015). https://doi.org/10.1093/mnras/stv714. arXiv:1412.5630

Tsutsui, R., Yonetoku, D., Nakamura, T., Takahashi, K., Morihara, Y.: Mon. Not. R. Astron. Soc. **431**, 1398 (2013a). https://doi.org/10.1093/mnras/stt262. arXiv:1208.0429

Tsutsui, R., Yonetoku, D., Nakamura, T., Takahashi, K., Morihara, Y.: Mon. Not. R. Astron. Soc. **431**(2), 1398 (2013b). https://doi.org/10.1093/mnras/stt262. arXiv:1208.0429

Tu, Z.L., Wang, F.Y.: Astrophys. J. **869**(2), 23 (2018). https://doi.org/10.3847/2041-8213/aaf4b8

Yonetoku, D., Murakami, T., Nakamura, T., Yamazaki, R., Inoue, A.K., Ioka, K.: Astrophys. J. **609**, 935 (2004). https://doi.org/10.1086/421285. arXiv:astro-ph/0309217

York, D.: Can. J. Phys. **44**, 1079 (1966)

York, D.: Earth Planet. Sci. Lett. **5**, 320 (1968). https://doi.org/10.1016/S0012-821X(68)80059-7

York, D., Evensen, N.M., Lopez, M.M., Delgado, J.D.B.: Am. J. Phys. **72**(3), 367 (2004). https://doi.org/10.1119/1.1632486

Zhang, B., Mészàros, P.: Int. J. Mod. Phys. A **19**, 2385 (2004). https://doi.org/10.1142/S0217751X0401746X. arXiv:astro-ph/0311321

Zitouni, H., Guessoum, N., Azzam, W.J.: Astrophys. Space Sci. **351**(1), 267 (2014). https://doi.org/10.1007/s10509-014-1839-5. arXiv:1611.05732

Zitouni, H., Guessoum, N., Azzam, W.J., Mochkovitch, R.: Astrophys. Space Sci. **357**(1), 7 (2015). https://doi.org/10.1007/s10509-015-2311-x. arXiv:1611.08907

Zitouni, H., Guessoum, N., AlQassimi, K.M., Alaryani, O.: Astrophys. Space Sci. **363**(11), 223 (2018). https://doi.org/10.1007/s10509-018-3449-0. arXiv:1810.04124